UNIVERSITY OF MISKOLC
FACULTY OF MECHANICAL ENGINEERING AND INFORMATICS

COMPLEX EVALUATION OF RESISTANCE SPOT WELDING TECHNOLOGIES FOR DUAL-PHASE AND MARTENSITIC STEELS

Booklet of PhD Theses

PREPARED BY:
SAHM ALDEN ANIS MOHAMMAD ABD AL AL
Civil Engineering (BSc),
Infrastructure Engineering (MSc)

ISTVÁN SÁLYI DOCTORAL SCHOOL
TOPIC FIELD OF ENGINEERING MATERIAL SCIENCE, PRODUCTION SYSTEMS AND PROCESSES
TOPIC GROUP OF MATERIALS ENGINEERING AND MECHANICAL TECHNOLOGY

Head of Doctoral School
Prof. Dr. Gabriella Vadászné Bognár
DSc, Full Professor

Head of Topic Group
Prof. Dr. János Lukács
CSc, PhD, Full Professor

Scientific Supervisor
Dr. Ákos Meilinger
PhD, Associate Professor

Scientific Cosupervisor
Prof. Dr. Marcell Gáspár
PhD, Full Professor

Miskolc
2025

JUDGING COMMITTEE

chair: Prof. Dr. Károly Jármai, DSc, Professor Emeritus, University of Miskolc

secretary: Dr. Judit Pap, PhD, Senior Lecturer, University of Miskolc

members: Dr. habil. Kornél Májlinger, PhD, Associate Professor, Budapest University of Technology and Economics

Prof. Dr. Tünde Kovács, PhD, Full Professor, Óbuda University

Dr. István Sztankovics, PhD, Associate Professor, University of Miskolc

OFFICIAL REVIEWERS

Prof. Dr. Gerald Wilhelm, PhD, Full Professor, Munich University of Applied Sciences

Dr. habil. Béla Palotás, PhD, Professor Emeritus, University of Dunaújváros

1. INTRODUCTION

Resistance spot welding (RSW) is a technique that joins overlapped metal sheets by generating heat driven by Joule law through electrical resistance as current flows between the sheets (Faying surface) under pressure from electrodes resulting in localized melting and formation of a fusion zone (FZ) [1]. The joining of Advanced High Strength Steel (AHSS) presents considerable challenges due to their high strength, susceptibility to cracking, and the adverse microstructural changes that occur during the welding process [2]. DP steel exhibits unique properties like continuous yielding, low yield-to-tensile strength ratio, and high initial work hardening rate [3][4] offering a balance between strength and ductility [5]. DP steel consists of martensite islands (α’) dispersed in a ferrite matrix (α) [6][7]. This composite microstructure allows DP steels to achieve high strength while maintaining good ductility [4].

MS steels are extremely high-strength steels, with a very high tensile strength (>1200 MPa), up to 1700 MPa with relatively low elongation [8]. MS steel is characterized by a predominantly martensitic microstructure, offering higher strength but reduced ductility compared to DP steels designed for applications requiring high strength in the automotive industry [9]. RSW process is often associated with a meaningful reduction in the mechanical properties and strength of the welded joint [10]. Understanding the effects of welding parameters on the thermal cycle (temperature-time) in RSW is crucial for optimizing these parameters and achieving a balance between the strength and ductility of the required high-performance spot joint [11]. In general, there are three important factors for evaluating the quality of RSW, which are the weld-nugget size, weld mechanical performance, and failure modes [12]. The RSW pulsation technological parameter is a method for regulating electrical pulses hence control generated heat and enhance joint reliability. Moreover, the size, microstructure, and hardness of the FZ and HAZ are influenced by the local thermal history and can be controlled by the pulse current [13].

The macrostructure of the RSW is divided into three main zones: the fusion zone (FZ), the heat-affected zone (HAZ), and the base metal (BM). The HAZ surrounds the FZ and undergoes solid-state phase transformations without melting [14]. It is subdivided into sub-zones with distinct temperature ranges each contributing differently to the overall mechanical behavior of the welded joint due to their distinct microstructural characteristics.

The base material microstructure serves as a reference point for comparing changes that occur during the RSW process. Understanding the initial microstructure is crucial for interpreting the transformations and property changes in the welded regions [5], using both optical microscopy and SEM offers a comprehensive understanding of the weld's microstructure and mechanical properties. In RSW of AHSS like DP and MS steels, the austenite can transform into martensite, bainite, or ferrite/perlite depending on the cooling rate and the hardenability of the steels [15] significantly influencing the phase transformations in the FZ and HAZ [3][4]. These transformations, along with the size and distribution of martensite, and gradual microstructural changes such as retained austenite and lower bainite in transition areas, critically affect the mechanical properties of the welded joint [16].

Martensite is a hard, brittle phase in steel formed by the rapid cooling of austenite, which traps carbon in the lattice, causing distortion and hardness, with its properties influenced by carbon content [16]. In DP and MS steels, a martensitic microstructure forms in the weld metal when the cooling time $t_{8/5}$ (time to cool from 800 °C to 500 °C) is less than 3 seconds [17], with rapid cooling rates typical of RSW intersecting only with the martensite start line, resulting in predominantly martensitic structures in the FZ and HAZ [5]; the critical cooling time extends with higher carbon equivalents, highlighting the influence of alloy composition and transformation temperatures on martensite formation and hardness [9].

Tempering characteristics of martensite in DP steels are similar to fully MS steel of comparable carbon content [7]. The extent of tempering/softening depends on the diffusion of carbon, controlled by temperature and time [7]. Steel composition, particularly carbon content and other alloying, affects the hardenability and transformation temperatures [9]. The FZ and coarse-grained heat affected zone (CGHAZ) exhibited peak hardness due to fresh martensite formation [18] while the HAZ showed a gradual hardness drop (softening) from ferrite/bainite formation or tempered martensite [14]. The softening is directly proportional to the martensite volume fraction (MVF) in the BM [4][17]. Controlling HAZ softening becomes a critical factor in producing high-performance welds in MS steel, as it directly impacts the overall strength and integrity of the welded structure [19].

During RSW, the steel is rapidly heated to temperatures above its melting point (> 1400 °C) in the FZ followed by subsequent rapid cooling, which occurs primarily through heat dissipation to the electrodes [9]. Heat dissipation in RSW involves conduction, where heat spreads through the metal sheets and welding electrodes influenced by their thermal conductivity; convection, which can be applicable if a water-cooling system is applied in electrodes; and radiation, which plays a minor role but can contribute to heat loss at higher temperatures [20]. Understanding the thermal history of RSW technologies is crucial for interpreting the microstructural changes that occur during welding [21], particularly the formation of martensite and its tempering [18]. The cooling rate in addition to composition significantly impacts the microstructure and properties of UHSSs [22].

Physical measuring the exact temperatures in RSW is quite challenging [23] due to the rapid thermal cycle, high welding currents that generate strong electromagnetic fields, and small vibrations. The data obtained from the measurement can be used to determine the peak temperature reached during the welding, the heating, and cooling rates, and the time spent at specific temperature ranges. The size of FZ and properties can be inferred from the temperature-time profile [24].

For many steels, especially high-strength steels used in automotive applications, the cooling rates in RSW can range from 10^3 to 10^4 °C/s [25]. Varying the second pulse current in a pulsed RSW schedule can modify the weld thermal cycle and alter cooling rates during welding [13]. Finite element analysis (FEA) simulations were applied to investigate the thermal cycles of RSW, and experimental techniques for correlating welding parameters with thermal history, microstructure, and mechanical properties [18]. Electro-thermal models combine electrical and thermal properties to show how electrical current influences heat generation within the workpieces.

During the welding process, the FZ undergoes complete melting and rapid solidification, resulting in a dendritic structure that grows directionally from the fusion line toward the center of the FZ [6], characterized by a fully martensitic structure with a columnar lath or needle-like morphology [26]. This transformation is facilitated by the high cooling rates inherent to the RSW process primarily due to the rapid cooling, which suppresses the formation of phases like ferrite or bainite. The HAZ exhibits a gradient of microstructural variations resulting from the differing peak temperatures and cooling rates experienced across its sub-zones during the welding thermal cycles [4].

The enhanced performance of 2-pulse joints is attributed to the FZ's randomly oriented grains with high-angle grain boundaries and the toughness improvement from martensite tempering [18]. 2-pulse welds exhibit a distinct microstructural division, with an inner fusion zone (FZ2) comprising coarse columnar grains similar to single pulse welds [27], and an outer recrystallized zone (Rex-zone) characterized by equiaxed prior austenite grains with coarser Bain groups and fewer high-angle grain boundaries resulting in lower hardness and residual strain, compared to inner fusion zone (FZ2) which affects crack initiation and propagation resistance [6].

Fatigue in vehicle **c**omponents arises from time-varying loads induced by road irregularities and vehicle dynamics. These stresses lead to the accumulation of damage over time, ultimately resulting in crack initiation and failure, especially in joints like spot welds [28]. Predicting joint performance in AHSS is complex, involving the interaction of geometrical factors, metallurgical properties, and loading mode [29].

The microstructure-driven fatigue performance of resistance spot welds is predominantly influenced by stress concentration and notch sensitivity rather than the base material's strength, with high-cycle fatigue behavior remaining largely consistent across different steel grades due to shared crack initiation and propagation mechanisms [30].

Crack initiation and propagation in high cycle fatigue (HCF) of RSW welded joints are governed by localized stress concentrations and microstructural heterogeneities, with fatigue cracks often originating at weld interfaces or notch tips due to metallurgical differences, while their growth path follows regions of reduced fracture toughness, such as tempered martensitic zones in the HAZ, particularly under cyclic loading conditions [31].

Fatigue life is significantly influenced by weld notch geometry, with larger nugget diameters and optimized notch root angles enhancing stress distribution and resistance to cyclic loading [32], while increased joint angles, smaller notch radii, and sharper notches elevate stress concentrations, accelerating crack growth and reducing fatigue performance [33]. Fatigue cracks in welded joints predominantly initiate at stress concentration points within the HAZ or FZ, propagating perpendicularly through the sheet thickness and extending in eyebrow shape outward along the FZ or base material, with crack pathways influenced by material properties, weld geometry, and cyclic loading conditions [34].

Fatigue cracks consistently initiate at an oxidized structure on the weld periphery, referred to as the "tongue." This tongue forms during the welding process when molten material is expelled and solidifies along the sheet interface [35].

The Charpy impact test is regarded as one of the most frequently used tests to evaluate the relative toughness of a material in a fast and economical way [36]. The Charpy impact test is a standard test to measure the impact energy (also referred to as notch toughness) absorbed by a material during fracture. Besides these, the developed impact test methods for RSW joints are investigating the impact-shear or impact-tensile properties, which do not perfectly show the behaviour of spot welds in case of real impact effect. The results of the performed dynamic tests and fracture tests showed that the failure mode of RSW joints of AHSS are very often interfacial or are only partial weld pull-out. This is presumably due to the fact that the welding parameters to be used during production are chosen on the basis of the results of conventional, quasi-static tests (shear-tensile, cross-tensile, peel, etc.) [36]. Typically, the side parts of a car chassis during a car crash suffer impact-bending. The impact velocity range can be very variable, in the case of low-speed car crash simulations it is less than 10 m/s [37]. The notch provides a point of stress concentration within the specimen and improves the reproducibility of the results [38]. The absorbed energy is computed by working out the potential energy lost by a pendulum by breaking a specimen [38]. This means that the dynamic characteristics of the whole structural element containing the welded joint can be determined, thus simulating the processes that take place during an actual collision [36][39].

The impact energy characterization of RSW specimen enhanced with additional instrumentation setup is designed to extract detailed mechanical data during impact testing. This approach often involves strain gauges mounted on the striker and a velocity measurement system to measure the load-time behavior as the specimen undergoes deformation and fracturing.

To achieve consistent and reproducible results, it is crucial to meticulously control all welding process variables so the testing process and the temperature conditions must be the same in all samples. Resistance spot welder machine calibration is a crucial process that ensures the welding equipment operates correctly and produces high-quality welds consistently [40][41]. Misalignment of the electrode or inconsistencies in electrode force can lead to irregularities in the nugget formation. These irregularities can complicate the measurement of nugget diameter, which is a critical parameter for assessing weld quality [42]. Geometrical deviation in RSW refers to the variations in the dimensions and positions of welds that occur during the welding process. Geometrical deviation can impact the failure characteristics of welded joints during mechanical testing. Variations in sample geometry, such as the dimensions and positioning of the FZ, can lead to stress concentrations, premature failures, and lower strength measurements.

2. PURPOSE OF THE DISSERTATION

Since the causes of mechanical changes resulting from the RSW process are varied and complex, this thesis aimed to investigate the resistance spot weldability of DP and MS steels, focusing on coveted RSW outcomes that demonstrate superior performance in the automotive industry. The study examined the microstructural evolution and its impact on mechanical properties. The research involved characterizing the microstructure of the weld nugget (WN) and HAZ using various techniques, including SEM, EBSD, and hardness mappings, to correlate specific microstructural features with mechanical properties determined by dynamic, quasi-static tests. In this research, the work builds upon existing literature in key areas, such as RSW parameter optimization and microstructural evolution. However, this approach is not applicable in all aspects, particularly where conflicting results exist such as the HCF behavior of AHSS or in areas that have either never been investigated or were explored a long time ago, such as RSW impact force performance and HCM. The challenges in the impact test are encountered in measuring the force as a function of time since a very high sample rate instrumentation in the testing device is required. To modify unwelcoming microstructural constituents, different in-process heat treatments were performed using a second pulse technological parameter. The heat input and cooling rates in HAZ sub-zones welded by single and double-pulse technology were measured physically and by a thermal simulator (SYSWELD). The challenge of capturing the very high seed RSW heating-cooling cycle is encountered, and the allocation of the thermocouple in a certain location is also made difficult by the small HAZ subzone. The HAZ was characterized in terms of microstructure and local mechanical properties. Martensite and ferrite content were microstructurally determined, and mechanical properties were evaluated through mechanical and microstructural testing on these single and double pulse samples, with the goal of determining the characteristics of the weld nugget and HAZ sub-zones for RSW joint integrity.

Based on the literature review, this research was undertaken to conduct comprehensive mechanical and microstructural examinations necessary for evaluating the RSW of AHSS for automotive applications. The specific aims of the research are as follows:

- Studying the effect of geometrical deviations during the preparation of RSW testing samples on the quasi-static tests of AHSS steel to determine the level of accuracy required to achieve consistent and reliable results.
- Determining the AHSS base material properties on the performance of RSW to enhance the integrity of spot welds under static, impact, and cyclic loading conditions.
- Examining the impact of optimizing welding parameters and welding technologies (1-pulse and 2-pulse) on the mechanical performance and microstructural transformations in RSW to achieve high-quality welds that meet required specifications.
- Measuring physically the heat cycle generated during RSW to understand the microstructural transformations occurring in the WN and the HAZ and validating the RSW heat cycle modeling.
- Exploring HCF loading and fatigue failure in AHSS to identify the key factors influencing RSW fatigue performance and durability.
- Measuring the force as a function of time to determine the absorbed impact energy in RSW and evaluate the behavior of spot joints under collision by implementing a new impact testing method.
- Evaluating the ability of RSW joints to withstand impact forces and analyzing impact failure under specific conditions.

3. METHODOLOGY

This dissertation focuses on the performance of RSW under various mechanical loading conditions, particularly in the context of its application in the automotive and aerospace industries. These industries often subject welded joints to complex combinations of loading modes, including tensile, shear, bending, cyclic, impact, and compound stresses. Understanding how RSW joints behave under such conditions is essential for ensuring structural safety and performance in real-world scenarios.

The scope of this study specifically targets Advanced High-Strength Steels (AHSS), which are widely used due to their superior strength-to-weight ratios and potential for lightweight design. A primary objective of this work is to investigate how different welding parameters influence the mechanical behavior and durability of RSW joints in AHSS.

To ensure a reliable and comprehensive analysis, the research was carried out in a series of logical and systematic steps. The first step involved establishing a consistent and repeatable sample preparation process for the RSW joints. This was critical in ensuring that the test results would be reliable and not influenced by inconsistencies in the weld quality.

Following sample preparation, the influence of various welding parameters such as current, time, and pulsation technology was studied through quasi-static mechanical tests. These included the cross-tension test and the tensile-shear test, both of which are commonly used to evaluate the strength of spot-welded joints. Additionally, macroscopic examinations and microhardness tests were performed to assess the weld nugget characteristics and hardness distribution across the welded zone.

After identifying the most optimal and reliable set of welding parameters from the quasi-static tests, dynamic loading conditions were introduced. These included fatigue and impact tests, designed to simulate real-world operational stresses. The objective of these dynamic tests was to evaluate the long-term performance and failure behavior of the welds under repetitive or sudden loads.

To deepen the understanding of microstructural evolution resulting from the RSW process, the thermal cycle of the weld was both physically measured and simulated. This helped to correlate welding parameters with resulting changes in the microstructure, which in turn affect the mechanical properties of the joint.

This study investigates the impact of geometrical deviations on the mechanical testing of RSW joints welded by 8.5 kA long-time welding parameter (see Table 1), particularly focusing on tensile shear and cross-tension tests of DP and MS steels. The primary aim is to establish guidelines for specimen geometry that enhance the reliability of test results, ensuring that failure modes observed during testing are reflective of the weld's inherent strength rather than artifacts caused by geometrical inconsistencies. The test samples, made from SSAB Docol DP600, DP800, DP1000, MS1200, and MS1400 steels, were all 1 mm in thickness. The research quantifies how variations in sample geometry such as misalignment, displacement, and deviations in FZ positioning affect load-displacement results, and failure modes.

To assess these effects, a series of tensile shear and cross-tension tests were conducted. Each test was grouped based on the type of geometrical deviation introduced, and each group was exposed to three distinct deviations. For the cross-tension test, the deviations included displacement along the sliding line (SL. disp.), angular misalignment (Ang. mis.), and displacement of the spot weld from the tension centerline (SW. disp.), with each deviation tested at three levels: 0.75 mm, 1.0 mm, and 2.0 mm for displacement, and 3°, 4°, and 8° for angular misalignment. For the tensile-shear test, the first group experienced parallel misalignment (Par. mis.) of one sheet from the centerline of the spot weld in the second sheet. Each group's results were compared to those of a standard sample with accurate geometry to isolate the effects of these deviations on the mechanical properties of the welds.

The sample preparation involved precise cutting and cleaning of the base material sheets, removing oils, grease, and oxides to ensure accurate weld placement and electrical resistance. A dimensionally accurate cross-tension test tool was created to apply controlled tensile forces to the RSW joints in a cross configuration for strength assessment. The RSW process itself was carried out using a TECNA 8007 resistance spot welder, controlled by a TE550 microprocessor-based welding unit, with copper chromium zirconium (CuCrZr) electrodes and a 5 mm spherical head diameter, optimized for the 1 mm sheet thickness.

For the calibration of the RSW machine, TECNA TE1700 RSW weld testers were used, ensuring that welding current, force, voltage, and energy inputs matched the desired standards, confirming the machine’s performance and reliability. The welding parameters were optimized to produce defect-free FZs, meeting the required mechanical and microstructural standards. The results indicated that failure always occurred at the crest of the deformation, reflecting the material's ductility in response to applied stresses, and demonstrating the influence of geometrical deviations on the consistency and reliability of test results.

Most notably, standard MS1400 samples (with no deviations) outperformed those with 2 mm misalignment and 8° angular deviation, emphasizing how even minor geometric imperfections can critically undermine weld strength in ultra-high-strength steels. Compared to the lower-grade DP steels and MS1200, MS1400’s results were more adversely affected by deviations, largely due to its lower ductility. This highlights the crucial need for tighter manufacturing tolerances when working with high-strength, low-ductility materials like MS1400 to preserve weld integrity.

The study investigates the impact of various welding parameters on the resistance spot welding of different steel grades, specifically DP and MS, aiming to optimize these parameters for better performance. The primary focus is on evaluating the macrostructure and mechanical properties of the welded joints, using tensile-shear (T-S) tests, optical macroscopic examinations, and microhardness measurements. The research explores three different welding technological parameters: short-time (5.8 kA), 2-pulse (6.4 kA), and long-time (8.5 kA), and compares the performance of MS1200 and MS1400 under these conditions. Table 1 showing the RSW parameter combinations.

Table 1. RSW parameters.

Welding technology	Weld current (kA)	Welding time (ms)	Cooling time (ms)	Pulse number	Welding force (kN)
Long time	8.5	320	-	1	5
2-pulse	6.4	120	300	2	3
Short time	5.8	240	-	1	3

Tensile-shear test results reveal that long-time welding (8.5 kA) leads to the highest peak loads, largest displacements, and the most significant FZ sizes, with pull-out failure modes indicating stronger welds. Conversely, short-time welding (5.8 kA) results in weaker joints, marked by lower peak loads and smaller displacements, with interfacial failure (IF) observed. The 2-pulse welding parameter offers moderate improvements in strength, displacement, and failure mode. Additionally, MS1200 exhibits slightly greater ductility than MS1400, with larger displacements, even though MS1400 demonstrates higher strength and load capacity.

Macrostructural and microhardness evaluations show softening in the weld zones, particularly in the softened heat-affected zones (SCHAZ and ICHAZ), where MS1200 and

MS1400 welded with 8.5 kA current displayed reductions in hardness. The 2-pulse parameter resulted in two softening zones, with a slight increase in hardness between them.

The long welding time was initially applied to determine the optimal welding condition that produced the best results in terms of joint strength and weld quality. Once the long-time welding produced the best results in terms of joint strength, it was consistently applied to all the investigated steel grades. This approach allowed for a controlled comparison to observe how different steel grades respond to the same optimized spot-welding condition, and to assess how the inherent properties of each material, particularly strength and ductility, influence the overall quality and performance of the welded joints. Microhardness testing confirms the relationship between the softening effect and base material strength, with the most significant softening in MS1400 and hardening in the fusion zone of DP600.

The study highlights that welding parameters have a more substantial effect on FZ size than the type of base material. All joints exhibited pull-out failure, indicating reliable weld integrity under tensile loading. The study demonstrates that welding current and time play critical roles in determining the mechanical properties of welded joints, with longer welding times and higher currents improving weld strength and fusion. Furthermore, the steel grade influences both the strength and ductility of the welded joints.

The study focuses on high-cycle fatigue (HCF) testing of RSW (RSW) joints made from various advanced steel grades, including dual-phase steels (DP600, DP800, DP1000) and martensitic steels (MS1200, MS1400), with the aim of evaluating their fatigue behavior and mechanical properties. The research investigates RSW joints geometry, particularly the notch (tongue), affect the performance and fatigue resistance of these welded joints. Additionally, the influence of steel grade on HCF performance is examined by comparing the fatigue life of joints made from different materials, all welded using the same long-time welding parameters.

The methodology follows the JSME S 002-1981 standard, which outlines a staircase method for determining the fatigue limit and endurance limit of materials under high-cycle conditions. In this study, lap shear samples of 1 mm thickness from each steel grade were prepared for fatigue testing, with twenty samples per grade to ensure reliability. The samples were welded using RSW techniques and subjected to tensile-tensile cyclic loading at room temperature. The MTS 322.41 electro-hydraulic universal test frame was used to apply a sinusoidal load with a load ratio of $R = 0.1$ and a frequency of 30 Hz. The load range and number of cycles to failure were plotted to generate the Load range-number cycle to failure (ΔL-N) curve, which is used to determine the material's endurance limit.

HCF testing results showed that DP steels had superior fatigue resistance compared to MS steels. As the grade of DP steel increased (DP600 < DP800 < DP1000), the fatigue resistance improved, with DP1000 exhibiting the highest load range and endurance limit. In contrast, MS1200 and MS1400 showed lower endurance limits, despite MS1400 having the highest base material strength. Figure 1. represents fatigue test data for the investigated materials

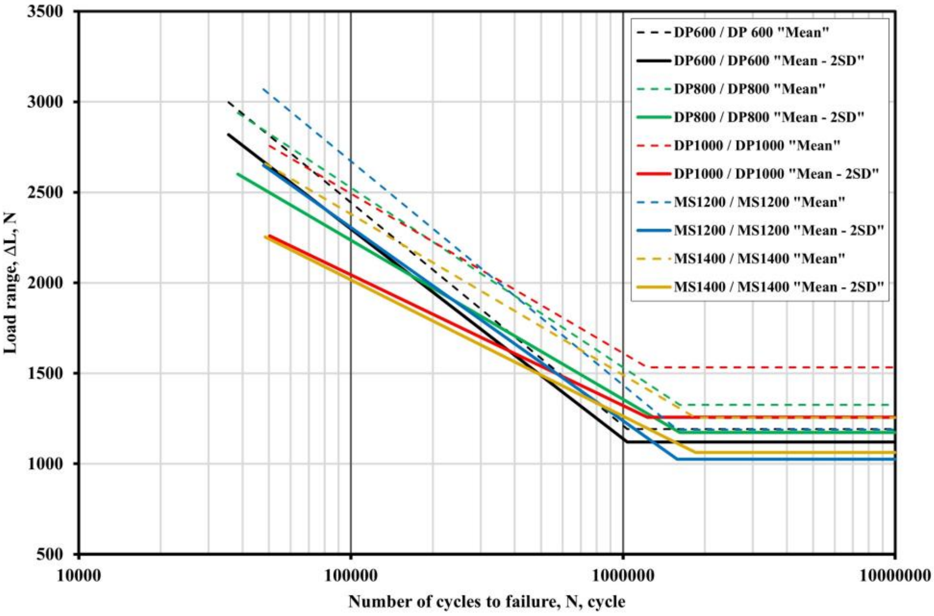

Figure 1. Load range-number cycle to failure (ΔL-N) curve.

A consistent fracture pattern was observed across all materials, with cracks typically initiating at the tongue and notch area within the FZ, where stress concentration and microstructural variations are most pronounced.

The fatigue crack growth analysis revealed that the cracks propagated through the HAZ, with the propagation path influenced by the material's hardness and toughness. The microhardness measurements at the crack initiation point confirmed that material grade significantly affects fatigue performance. The findings suggest that DP steels are more suitable for components subjected to cyclic loads, offering a better balance of fatigue resistance and ductility, while MS steels should be avoided in such applications due to their lower fatigue resistance. The research underscores the importance of selecting appropriate materials for applications subjected to cyclic loading, with DP steels being the preferred choice for durability and safety in automotive and structural applications.

This study applied a new method for testing the dynamic loading capacity of RSW joints made from dual-phase (DP) steels, specifically DP600 and DP800. The primary goal is to evaluate the resistance of these welded joints under impact loading conditions, using a developed instrumented impact-bending test. This method quantifies the behavior of RSW joints subjected to forces similar to those experienced during car crashes (collision), providing more precise numerical data compared to traditional methods. The study compares different welding parameters, including long-time welding, short-time welding, and 2-pulse welding, to assess their impact on dynamic loading performance.

The testing method involves an instrumented setup for the impact-bending test, where a pendulum swings down to strike the specimen. A strain gauge attached to the striker measures the applied force, while a photogate tracks the time intervals of the pendulum's motion. The data from the strain gauge and photogate are processed by an amplifier and oscilloscope to generate a force-time diagram, which provides insights into the force, impact duration, and energy absorption during fracture. The modified test setup uses a pendulum with a reduced weight, offering a maximum impact energy of 118.25 J, more suitable for the 1 mm thick overlapped joints of high-strength DP steels.

Microhardness examinations were performed to identify failure locations in the welded joints. The results show that with long-time and 2-pulse welding, the fracture occurs in the softened area of the HAZ. In contrast, short-time welding results in fracture starting from the edge of the fusion zone (FZ).

The findings reveal that the steel grade and welding technology influences the dynamic loading resistance of RSW joints. Among all the investigated steel grades, DP1000 exhibited the highest impact resistance when welded using the long-time welding parameter (see Figure 2). Long-time welding generally produces the best performance (see Figure 3), as it results in a more robust joint, while short-time welding leads to the poorest outcomes due to imperfect fusion and a smaller nugget diameter.

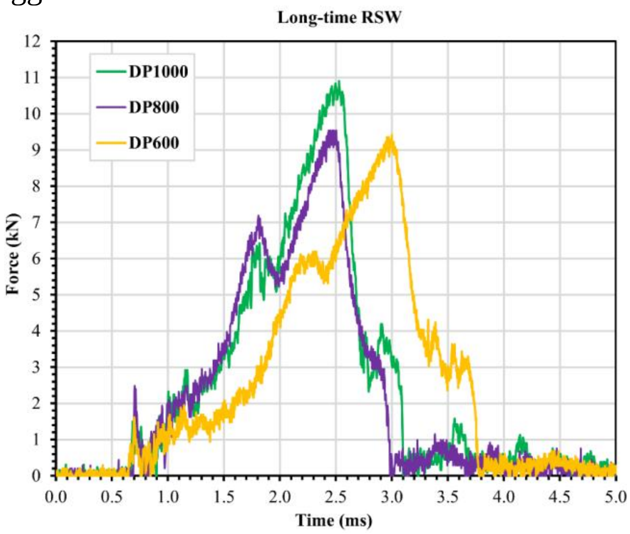

Figure 2. Impact force – time curves on samples welded by Long-time RSW parameter

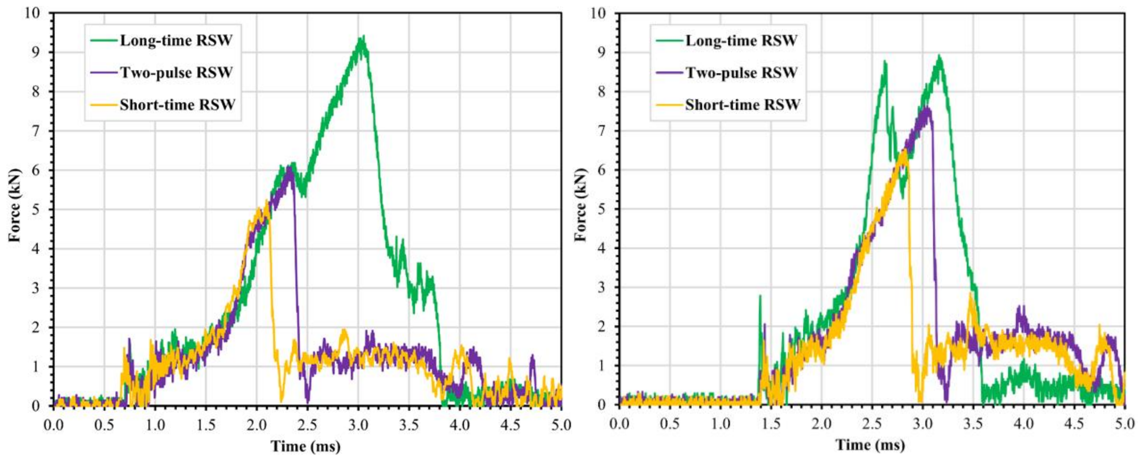

Figure 3. Impact force – time curves on DP600 (left) and DP600 (right) welded by different welding parameters

The study highlights the importance of optimizing welding parameters to ensure better performance of RSW joints under dynamic loading conditions, particularly for applications like automotive structures where crash resistance is crucial.

The research focused on measuring and simulating the heat cycle in RSW to understand the resulting changes in mechanical properties and microstructural formations in high-strength steel sheets. Moreover, to contribute optimizing RSW processes, particularly in the AHSS, where controlling the HAZ and microstructural changes is critical. Accurate cooling rate measurements, including $t_{8/5}$ cooling time, are crucial to predict microstructural evolution, but challenges arise due to high temperature gradients and the small size of the weld and HAZ.

These challenges were compounded by the electromagnetic interference from the alternating current during the welding process, which caused noise in thermocouple readings. The study employed various techniques to mitigate this interference, such as filtering the data and minimizing thermocouple exposure to the magnetic field.

The experimental setup involved 1 mm thick Docol MS1400 steel sheets. The geometry of the specimens consisted of a base sheet (100×30 mm), a thermocouple sheet, and a confining sheet (both 50×30 mm). The a micro K-type (Chromel/Alumel) thermocouple, was welded into the cross-section of the sheet using a specialized micro-welding device. Several thermocouples were embedded within the base material of the HAZ, placed away from the weld center to avoid interference from high currents and electromagnetic fields. These thermocouples measured thermal cycles in different zones of the HAZ: UCHAZ, ICHAZ, and SCHAZ. To ensure accuracy, the distance between the thermocouple and the FZ was measured, considering the symmetry of heat conduction from the nugget.

Two welding technologies were employed for the experiments: long-time single pulse welding and 2-pulse welding. Thermal measurements were taken using the HBM Spider8 modular acquisition system, which provided high-speed data acquisition suited for rapid temperature changes. The results showed significant differences between the two welding methods. In 2-pulse welding, the cooling rate in the UCHAZ was five times faster than in long-time welding, leading to more controlled grain structures in the HAZ. The cooling time from 800 °C to 500 °C ($t_{8/5}$) was also much shorter in 2-pulse welding compared to long-time welding (see Figure 4). The FZ in 2-pulse welding was smaller with finer grains, while long-time welding produced a broader FZ with coarser grains due to prolonged heating.

The study also validated the finite element model (FEM) by these experimental findings in order to adopt the simulation in RSW design, it is essential to recognize its advantages in terms of cost-efficiency and speed compared to physical testing. The model simulated temperature distributions for both welding methods, using a 2D axisymmetric model developed with SYSWELD software taking into account welding parameters, base metal properties, and the boundary conditions. As shown in Figure 4. the FEM simulation showed similar temperature profiles to the experimental results, with long-time welding leading to a broader temperature distribution and slower cooling, while 2-pulse welding exhibited faster cooling and a smaller temperature distribution. The agreement between the simulation and physical measurements, particularly in the HAZ subzones, validated the accuracy of the FEM model and demonstrated its potential for predicting the thermal behavior of RSW processes.

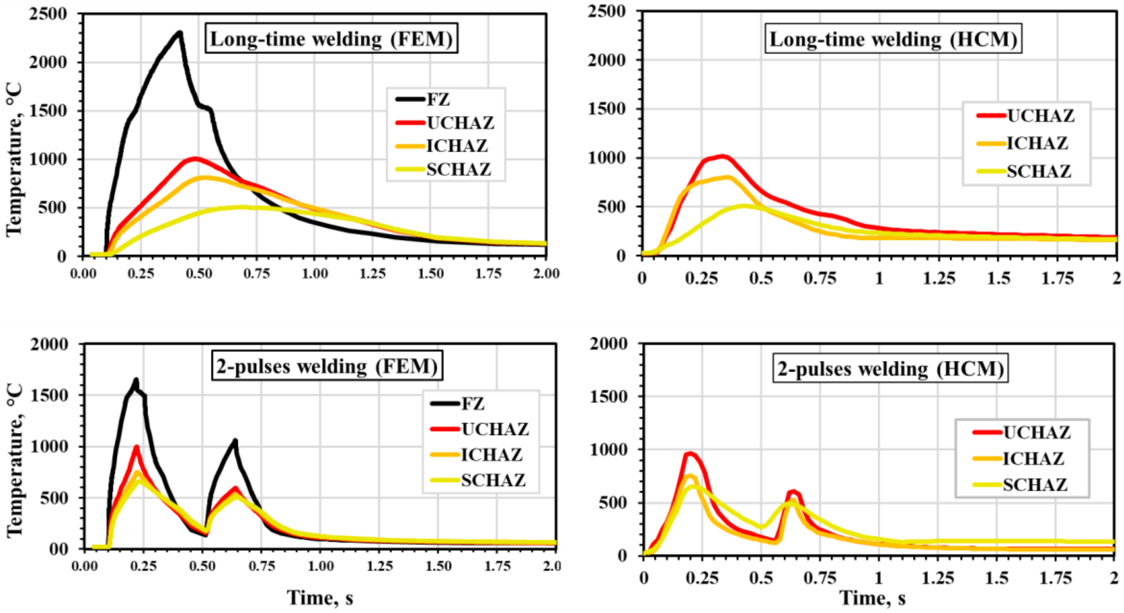

Figure 4. HCM of the long-time and 2-pulse RSW using FEM (Left), and physical HCM (Right)

The study provides a comprehensive approach to measuring and modeling the heat cycle during RSW. It highlights the significant differences in the HAZ between long-time and 2-pulse welding methods and validates the use of FEM simulations to predict the thermal behavior of RSW with good accuracy.

The study highlighted the impact of different thermal cycles on the microstructure and mechanical properties of MS steel joints, with notable differences between long-time and 2-pulse RSW welding methods. The study investigates the microstructural evolution of 1400 MPa, with the aim to provide insights into the microstructural changes induced by these welding techniques. Docol 1400M steel sheets, with a thickness of 1 mm, were used as the base material, and various welding parameters for both techniques were detailed. The research focused on comparing the microstructural characteristics and mechanical properties of welded joints.

For microstructural characterization, a field-emission scanning electron microscope (FESEM) equipped with electron backscatter diffraction (EBSD) was employed. The EBSD data were analyzed using the Image Quality (IQ) method, which enabled the identification and quantification of different microstructural phases, such as martensite and bainite, based on their distinct IQ values and the grain size were measured by FESEM.

The results showed significant differences between long-time and 2-pulse welding. For long-time welding, the microstructure was dominated by martensite and tempered martensite in the FZ, as well as in the subzones of the HAZ. Through the analysis of the recorded thermal cycle reveals the phase transformations within the material. At elevated temperatures, the microstructure forms austenite, which then transforms into martensite during rapid cooling demonstrating a typical thermal response under fast quenching conditions. The rapid cooling from high peak temperatures resulted in martensitic transformation, with variations in the cooling rates across different regions, including the un-tempered, fully tempered, and partially tempered martensite. In contrast, the 2-pulse welding introduced a second thermal cycle that divided the FZ into two regions: FZ2 (inner FZ) and the Rex-zone (outer FZ). These regions showed distinct microstructural features, such as martensite and bainite, as well as different cooling and heating rates from the second pulse.

Figure 5 showing the EBSD-IQ analyses and revealed that the 2-pulse welding resulted in a lower percentage of martensite compared to long-time welding, especially in the FZ2 region, where a significant amount of bainite was formed. Additionally, the hardness measurements indicated that the 2-pulse welded joint exhibited lower hardness values in the UCHAZ due to the formation of bainite, which softened the material. In the ICHAZ, the 2-pulse welding resulted in slightly higher hardness compared to long-time welding due to the presence of more martensite.

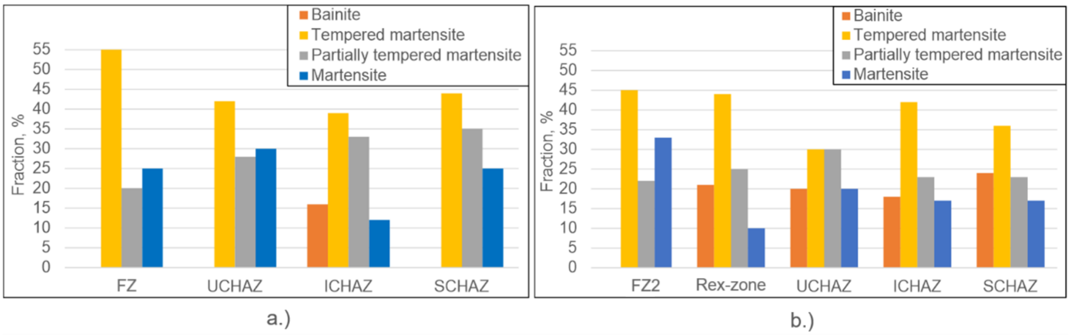

Figure 5. Fractions of different microstructural constituents in the subzones of RSW joints: a.) Long-time welding, b.) 2-pulse welding.

As shown in Figure 6. the grain size measurements revealed only minor differences between the two welding methods in the HAZ regions, with the 2-pulse welding producing larger grain sizes in the Rex-zone and smaller grain sizes in the FZ2. The grain size distributions in the FZ were more distinct in the 2-pulse welding, with a clear distinction between the two FZ regions.

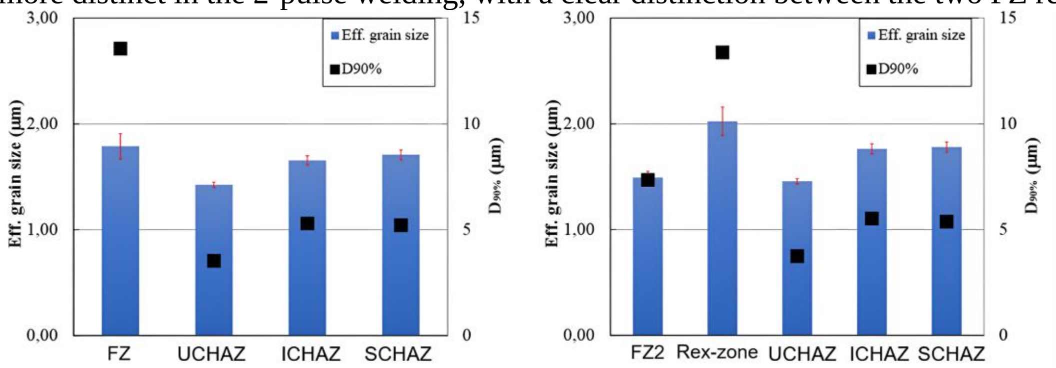

Figure 6. Grain sizes of the subzones: a.) long-time welding, b.) 2-pulse welding.

By combining experimental testing with thermal simulations and metallurgical evaluations, this methodology offers a robust framework for evaluating the reliability and performance of RSW joints in AHSS under realistic service conditions. The structured approach ensures that findings are not only scientifically rigorous but also practically applicable in industrial design and manufacturing processes.

4. SUMMARY AND INDUSTRIAL UTILIZATION

RSW is a key joining method in the automotive and aerospace industries, valued for its efficiency, speed, and ability to create strong joints in sheet metal structures. The rise of AHSS is crucial for reducing vehicle weight while maintaining crashworthiness, particularly in electric vehicles (EVs), which are significantly heavier due to their batteries. However, welding AHSS poses challenges due to its high hardness and heat sensitivity, necessitating the development of optimized RSW techniques. The performance of spot welds depends on stress conditions, which vary across vehicle and aircraft structures. Engineers must carefully select AHSS grades and tailor welding parameters to balance strength, ductility, impact, and fatigue resistance. This research provides valuable insights into the RSW of DP and MS steels, with applications extending beyond automotive and aerospace to industries, where AHSS is widely used.

Optimizing welding parameters is crucial for enhancing joint strength, durability, and defect prevention in RSW focuses on welding current, time, force, and pulsation technology to improve weld quality, particularly in AHSS. By controlling the RSW geometry, failure mode and HAZ softening, these optimizations ensure superior mechanical performance. Optimizing sample quality to enhance the accuracy of predictive models, improve welding techniques, and refine spot weld designs for AHSS in automotive applications. The research highlights the importance of sample geometry in determining mechanical properties and failure behavior. By precisely controlling these factors, engineers can improve weld performance, ensuring durability and consistency in both research and industrial-scale production.

Simulating heat cycles and validating them via physical measurements play a crucial role in optimizing RSW. FEM enables engineers to develop predictive models that refine welding parameters, minimize experimental costs, and enhance efficiency in industrial applications. By analyzing thermal history, engineers can optimize cooling rates, particularly in requiring precise thermal control. It underscores the difference between of long-time weld and 2-pulse RSW in refining weld microstructures in MS1400 steel, enhancing mechanical properties, and ensuring long-term structural reliability. Advanced microstructural characterization technologies, reveal key phase transformations and grain refinement processes in the FZ and HAZ, emphasizing the role of martensite and ferrite distribution in determining weld strength. This knowledge aids in the development of next-generation AHSS with improved weldability and fatigue resistance, supporting safer and more durable engineering designs.

The fatigue performance of HCF in RSW for AHSS is influenced by a combination of factors, primarily the steel grade and weld geometry so it essential to carefully consider both material selection and welding design in engineering automotive applications.To understand the behavior of RSW in DP steels during collisions in automotive engineering, instrumented impact testing serves as a sophisticated method to evaluate dynamic fracture behavior, capturing real-time data on how materials respond to sudden impact forces.

The base metal's is another essential factor that impacts the final properties of the weld. By integrating welding parameters, material properties, and geometrical factors,

The complexity in evaluating RSW of AHSS necessitates rigorous pre-design analysis of weld locations to account for variable mechanical demands. AHSS welding parameters and multi-pulse welding techniques, must be applied for each application due to the material’s hardenability, and susceptibility to localized stress concentrations. These factors, combined with site-specific loading conditions (static, dynamic, or combined stresses), complicate joint design. Achieving reliable and consistant RSW samples, is the demand of the mechanical and microstructural standardized testing to evaluate failure modes, weld geometry, and base metal interactions. Additionally, HCM and simulation can refine parameters to balance production efficiency with joint integrity.

5. NEW SCIENTIFIC RESULTS – THESES

T1. After investigating the effect of the geometrical deviation on tensile-shear (T-S) and cross-tension (C-T) tests of resistance spot welded under consistent conditions, the following was found (4) (8):

a. The results revealed that geometrical deviations have no significant influence on the strength, displacement, and failure mode for DP600, DP800, DP1000, and MS1200.

b. In contrast, MS1400 samples displayed reduced performance, with 2 mm and 8° degrees deviations showing a noticeable drop in the strength and displacement, while the failure mode showed more response to the geometrical deviation compared to the standard sample, proving that the higher strength of steel is more likely to be affected by the geometrical deviation and suggesting the importance of precise geometry of samples.

T2. The effects of welding parameters and base metal strength on the tensile-shear (T-S) test performance of resistance spot welding (RSW) were investigated and found (2) (3) (9) (17):

a. The comparative analysis of long-time, 2-pulse, and short-time RSW technologies on martensitic steels (MS1200 and MS1400) revealed that, despite all methods induced relatively similar softening values, the long-time welding emerged as the most effective welding technology, producing superior fusion zones (FZ) with the largest diameters, optimal strength, and favorable pull-out failure modes compared to 2-pulse and short time RSW. The findings suggest that welding parameters technologies play critical role in determining RSW T-S strength.

b. The comparative assessment of dual-phase (DP) and martensitic (MS) steels welded using the long-time resistance spot welding (RSW) process revealed that, while martensitic steels (MS1200 and MS1400) exhibited pronounced softening in the heat-affected zone (HAZ), they achieved the highest T-S strength and the lowest displacement. In contrast, dual-phase steels (DP600, DP800, and DP1000) demonstrated greater displacement before failure and lower T-S strength, with minimal softening observed only in DP1000. The findings suggest that base metal strength play critical role in determining RSW T-S strength.

T3. The high cycle fatigue (HCF) demonstrated consistent heat-affected zone (HAZ) failure modes within the two groups, dual-phase (DP) and martensitic (MS) steels. The steel grade significantly influences HCF behavior, as different grades exhibit varying hardness levels, which directly affect their fatigue performance. The HCF performance in case of mean-2 standard deviation (mean-2SD) follows a sequential trend supported by hardness measurements in the tongue (crack initiation zone). Specifically, lower hardness in this region corresponds to a lower endurance limit force (MS1200 and MS1400), while higher hardness corresponds to a higher endurance limit force (DP600, DP800, and DP1000) leads to improved fatigue resistance (5) (16).

T4. Based on the experimental results, by the developed impact-bending test method on dual-phase (DP) steels the different resistance spot welding (RSW) technologies and base materials can be effectively compared. For acceptable results, the plug diameter should be under 5.1 mm, as larger diameters may cause base material failure (7).

a. The welding technique and steel grade play crucial roles in determining the impact energy of resistance spot welds. Long-time welding consistently outperforms other methods (2-pulse and short-time), producing the highest impact energy and force across all tested steel grades. Additionally, while DP600 and DP1000 exhibit similar impact energy levels, DP1000's superior impact force suggests greater overall impact safety.

b. The comparison of the impact energy and impact force between DP600 and DP800, reveals notable differences influenced by the welding technology used. In the long-time welding, the impact energy of DP600 is approximately 5% higher than DP800's. In contrast, for the 2-pulse, DP600 records a significant reduction in energy absorption compared to DP800 and the short-time welding showed a similar trend for 2-pulse RSW. These variations highlight the influence of material properties and welding parameter on joint performance in impact loading resistance.

T5. A physical heat cycle measuring method was further developed to physically measure the heat cycle in depth within the heat-affected subzones of resistance spot welding (RSW). The method accurately assesses the heat cycle facilitating the correlation between thermal cycles and microstructural transformations thus optimizing welding parameters. The recorded heat cycle for both long-time and 2-pulse RSW revealed significant differences in thermal profiles, including temperature gradients, cooling rates, and peak temperatures across the heat-affected subzones of both technologies. In the upper critical heat-affected zone (UCHAZ), the $t_{8/5}$ (time to cool from 800°C to 500°C) in the 2-pulse RSW process was observed to be five times faster than that of long-time welding. The measured heat cycle closely correlates with finite element modeling (FEM), providing a reliable validation of the simulation's accuracy in predicting thermal behavior during welding (6) (10) (14).

T6. A comparative microstructural analysis of MS1400 steel long-time and 2-pulse welding revealed notable differences in microstructural evolution (15).

a. The microstructure of weld zones varies significantly between long-time and 2-pulse welding. In the long-time, bainite appeared only in the inter-critical heat subzone (ICHAZ). However, in the 2-pulse welding, bainite formed in all heat-affected subzones and the recrystallized zone (Rex-zone), except the inner fusion zone. Notably, bainite fraction reduced the overall martensite fraction compared to zones without bainite, influencing the mechanical properties between long-time and 2-pulse spot joint welding

b. The effect of welding parameters on 90% of the cumulative grain size distribution ($D_{90\%}$) reveals a tendency for different heat-affected subzones to exhibit significant similarity in effective grain size between long-time and 2-pulse welding technologies. In long-time welding, the fusion zone (FZ) has the largest grain size, while in 2-pulse welding, the Rex-zone experiences the most coarsening. Notably, 2-pulse welding results in a distinct grain size variation within the FZ, forming an outer (Rex-zone) and inner fusion zone (FZ2) zones with different microstructural characteristics.

6. LIST OF PUBLICATIONS RELATED TO THE TOPIC OF THE RESEARCH FIELD

IN ENGLISH

(1) S. Alden Abd Al Al, M. Gáspár, and Á. Meilinger, “Properties of Hybrid Aluminium-Steel Joints Made by Resistance Spot Welding,” Defect and Diffusion Forum, vol. 416. Trans Tech Publications, Ltd., pp. 131–138, May 27, 2022. doi: 10.4028/p-3099yq.

(2) S. alden Abd al al and Á. Meilinger, “Investigation of Resistance Spot Welded Joints Made on Ultra-high-Strength Steel Sheets,” Lecture Notes in Mechanical Engineering. Springer International Publishing, pp. 981–994, Sep. 10, 2022. doi: 10.1007/978-3-031-15211-5_82.

(3) S. alden Abd al al and Á. Meilinger, "Development of resistance spot welding technology on ultra-high strength steel sheets: Ellenállás-ponthegesztési technológia fejlesztése ultra-nagyszilárdságú acélokhoz," in XXXI. Nemzetközi Hegesztési Konferencia, J. Gáti, Ed. Budapest, Hungary: Hungarian Welding Association, 2022, pp. 113–123.

(4) S. Alden Abd al al, M. Fodorné Cserépi, M. Gáspár, and Á. Meilinger, “Optimizing Sample Preparation for Destructive Testing in Resistance Spot Welding,” Journal of Physics: Conference Series, vol. 2848, no. 1. IOP Publishing, p. 012005, Sep. 01, 2024. doi: 10.1088/1742-6596/2848/1/012005.

(5) S. Alden. Abd Al Al, Á. Meilinger, M. Gáspár, and J. Lukács, “High Cycle Fatigue Testing of Lap Shear RSW Joints from Martensitic MS1400 Steel Sheets,” Materials Science Forum, vol. 1095. Trans Tech Publications, Ltd., pp. 139–151, Aug. 18, 2023. doi: 10.4028/p-o9mwsq.

(6) S. Alden Abd Al Al, Á. Meilinger, and M. Gáspár, “Physical Heat Cycle Measurement of Resistance Spot Welding,” Key Engineering Materials, vol. 989. Trans Tech Publications, Ltd., pp. 65–75, Oct. 28, 2024. doi: 10.4028/p-tb0owj.

(7) Á. Meilinger, L. Prém, S. A. Abd Al Al, and M. Gáspár, “Comparison of RSW technologies on DP steels with modified instrumented Charpy impact test,” Welding in the World, vol. 67, no. 8. Springer Science and Business Media LLC, pp. 1911–1922, Apr. 24, 2023. doi: 10.1007/s40194-023-01526-2.

(8) S. Alden Abd Al Al and M. Gáspár, "The impact of geometrical deviation on specimen testing for MS1400 martensitic steel in RSW," in XXXII. Nemzetközi Hegesztési Konferencia: Konferencia Kiadvány, J. Gáti and M. Gáspár, Eds., 2024, pp. 67–87.

(9) S. Alden Abd Al Al, C. M. Fodorné, M. Gáspár, and Á. Meilinger, "Resistance spot welding and dissimilar joining of automotive high-strength steels and aluminium alloys," GÉP, vol. 74, no. 4, pp. 73–76, 2023.

(10) S. alden Abd al al and Á. Meilinger, "Thermal Simulation of Resistance Spot Welding in Case of DP600 Steel," in Kutatási eredmények a Miskolci Egyetem Gépészmérnöki és Informatikai Karának Anyagszerkezettani és Anyagtechnológiai Intézetében, J. Kovács

and J. Lukács, Eds. Miskolc, Hungary: Miskolci Egyetem, Gépészmérnöki és Informatikai Kar, Anyagszerkezettani és Anyagtechnológiai Intézet, 2024, pp. 131–142.

(11) N. Tanuj, R. P. S. Sisodia, and S. alden Abd al al, "Experimental investigation of CMT welding parameters for DP1000 butt joints," Diáktudomány: A Miskolci Egyetem Tudományos Diákköri Munkáiból, vol. 17, pp. 79–87, 2024.

(12) M. Alhafadhi, M. Alsigar, Z. A. Oudah, Z. Bézi, S. alden Abd al al, and P. R. Reddy, "Influence of heat input and preheating on residual stresses in pipe weld," Pollack Periodica: An International Journal for Engineering and Information Sciences, vol. 19, no. 2, pp. 42–47, 2024.

IN HUNGARIAN

(13) M. Gáspár, S. alden Abd al al, and L. Gyura, "Lángegyengetési hőciklusok hatása az S1100M acél tulajdonságaira," in Kutatási eredmények a Miskolci Egyetem Gépészmérnöki és Informatikai Karának Anyagszerkezettani és Anyagtechnológiai Intézetében, J. Kovács and J. Lukács, Eds. Miskolc, Hungary: Miskolci Egyetem, Gépészmérnöki és Informatikai Kar, Anyagszerkezettani és Anyagtechnológiai Intézet, 2024, pp. 119–130.

(14) S. alden Abd al al and Á. Meilinger, "Hegesztési hőciklusok mérése különböző ellenállás-ponthegesztési technológiák esetén," in Kutatási eredmények a Miskolci Egyetem Gépészmérnöki és Informatikai Karának Anyagszerkezettani és Anyagtechnológiai Intézetében, Zs. Koncsik and J. Lukács, Eds. Miskolc, Hungary: Miskolci Egyetem, Gépészmérnöki és Informatikai Kar, Anyagszerkezettani és Anyagtechnológiai Intézet, 2023, pp. 95–106.

(15) S. Alden Abd Al Al. and Á. Meilinger, "Az impulzustechnika hatása az MS1400 alapanyagon végzett ellenállás-ponthegesztett kötések szövetszerkezetére," in Kutatási eredmények a Miskolci Egyetem Gépészmérnöki és Informatikai Karának Anyagszerkezettani és Anyagtechnológiai Intézetében, J. Kovács and J. Lukács, Eds. Miskolc, Hungary: Miskolci Egyetem, Gépészmérnöki és Informatikai Kar, Anyagszerkezettani és Anyagtechnológiai Intézet, 2024, pp. 85–94.

(16) S. Alden Abd Al Al, Á. Meilinger, M. Gáspár, and J. Lukács, "Martenzites és kettős-fázisú acéllemezek ellenállás-ponthegesztett kötéseinek nagyciklusú fárasztóvizsgálatai," in Kutatási eredmények a Miskolci Egyetem Gépészmérnöki és Informatikai Karának Anyagszerkezettani és Anyagtechnológiai Intézetében, J. Kovács and J. Lukács, Eds., Miskolc, Hungary: Miskolci Egyetem, Gépészmérnöki és Informatikai Kar, Anyagszerkezettani és Anyagtechnológiai Intézet, 2024, pp. 107–118.

(17) Á. Meilinger and S. alden Abd al al, "Ellenállás-ponthegesztési technológia fejlesztése ultra-nagyszilárdságú acélokhoz," Hegesztéstechnika, vol. 35, no. 1, pp. 35–41, 2024.

PRESENTATIONS

(18) Á. Meilinger, S. alden Abd al al , P. Kovács, J. Lukács, and M. Fodorné Cserépi, "The behavior of RSW and clinched joints from similar and dissimilar automotive materials under different loading conditions," Paper: III-2114-23, 2023.

7. LITERATURE CITED IN THE THESES BOOKLET

[1] R. Sreenivasulu, “Joining of Dissimilar alloy Sheets (Al 6063&AISI 304) during Resistance Spot Welding Process: A Feasibility Study for Automotive industry,” *Independent Journal of Management & Production*, vol. 5, no. 4, Dec. 2014, doi: 10.14807/ijmp.v5i4.231.

[2] P. Kah, M. Pirinen, R. Suoranta, and J. Martikainen, “Welding of ultra high strength steels,” in *Advanced Materials Research*, 2014, pp. 357–365. doi: 10.4028/www.scientific.net/AMR.849.357.

[3] S. S. Nayak, Y. Zhou, V. H. Baltazar Hernandez, and E. Biro, “Resistance spot welding of dual-phase steels: Heat affected zone softening and tensile properties,” *ASM Proceedings of the International Conference: Trends in Welding Research*, pp. 641–649, 2013.

[4] H. L. Jaber, M. Pouranvari, R. K. Salim, F. A. Hashim, and S. P. H. Marashi, “Peak load and energy absorption of DP600 advanced steel resistance spot welds,” *Ironmaking and Steelmaking*, vol. 44, no. 9, pp. 699–706, Oct. 2017, doi: 10.1080/03019233.2016.1229880.

[5] C. Rajarajan, P. Sivaraj, and V. Balasubramanian, “Microstructural analysis of weld nugget properties on resistance spot-welded advance high strength dual phase (α+α /) steel joints,” *Mater Res Express*, vol. 7, no. 1, 2020, doi: 10.1088/2053-1591/ab654d.

[6] A. Chabok, E. van der Aa, J. T. M. De Hosson, and Y. T. Pei, “Mechanical behavior and failure mechanism of resistance spot welded DP1000 dual phase steel,” *Mater Des*, vol. 124, pp. 171–182, 2017, doi: 10.1016/j.matdes.2017.03.070.

[7] V. H. Baltazar Hernandez, S. S. Nayak, and Y. Zhou, “Tempering of martensite in dual-phase steels and its effects on softening behavior,” *Metall Mater Trans A Phys Metall Mater Sci*, vol. 42, no. 10, pp. 3115–3129, Oct. 2011, doi: 10.1007/s11661-011-0739-3.

[8] M. Kekik, F. Özen, E. İlhan, and S. Aslanlar, “Microstructural Evaluation and Influence of Welding Parameters on Electrode Plunge Depth in Resistance Spot Welded Dissimilar DP800HF/1200M Steel Joints,” *Academic Platform Journal of Engineering and Science*, vol. 9, no. 2, pp. 284–291, May 2021, doi: 10.21541/apjes.859623.

[9] N. Nadimi, M. Pouranvari, R. Ansari, and M. Pouranvari, “Understanding fusion zone hardness in resistance spot welds for advanced high strength steels: Strengthening mechanisms and data-driven modeling,” *Journal of Materials Research and Technology*, vol. 26, pp. 5549–5565, Sep. 2023, doi: 10.1016/j.jmrt.2023.08.251.

[10] A. R. H. Midawi *et al.*, “A novel technique to measure the local mechanical properties of third generation advanced high strength steel resistance spot welds,” *Forces in Mechanics*, vol. 9, Dec. 2022, doi: 10.1016/j.finmec.2022.100150.

[11] P. Zhang, J. Xie, Y. X. Wang, and J. Q. Chen, “Effects of welding parameters on mechanical properties and microstructure of resistance spot welded DP600 joints,” *Science and Technology of Welding and Joining*, vol. 16, no. 7, pp. 567–574, Oct. 2011, doi: 10.1179/136217110X12813393169732.

[12] Y. Li, H. Tang, and R. Lai, “Microstructure and mechanical performance of resistance spot welded martensitic advanced high strength steel,” *Processes*, vol. 9, no. 6, Jun. 2021, doi: 10.3390/pr9061021.

[13] L. Khan, M. L. Kunts, Y. Zhou, K. Chan, and N. Scotchmer, “Monitoring the Effect of RSW Pulsing on AHSS using FEA (SORPAS) Software.”

[14] X. Wan, Y. Wang, and P. Zhang, “Effects of welding schedules on resistance spot welding of DP600 steel,” *ISIJ International*, vol. 54, no. 10, pp. 2375–2379, 2014, doi: 10.2355/isijinternational.54.2375.
[15] K. Aydin, M. Hidiroglu, and N. Kahraman, “Characterization of the Welding Zone of Automotive Sheets of Different Thickness (DP600 and DP800) Joined by Resistance Spot Welding,” *Transactions of the Indian Institute of Metals*, vol. 75, no. 5, pp. 1279–1291, 2022, doi: 10.1007/s12666-021-02482-5.
[16] A. Chabok, E. van der Aa, and Y. Pei, “A study on the effect of chemical composition on the microstructural characteristics and mechanical performance of DP1000 resistance spot welds,” *Materials Science and Engineering: A*, vol. 788, no. April, p. 139501, 2020, doi: 10.1016/j.msea.2020.139501.
[17] E. Javaheri, J. Lubritz, B. Graf, and M. Rethmeier, “Mechanical properties characterization of welded automotive steels,” *Metals (Basel)*, vol. 10, no. 1, pp. 1–19, 2020, doi: 10.3390/met10010001.
[18] I. A. Soomro, S. R. Pedapati, and M. Awang, “Optimization of postweld tempering pulse parameters for maximum load bearing and failure energy absorption in dual phase (DP590) steel resistance spot welds,” *Materials Science and Engineering: A*, vol. 803, Jan. 2021, doi: 10.1016/j.msea.2020.140713.
[19] M. Tamizi, M. Pouranvari, and M. Movahedi, “The Role of HAZ Softening on Cross-Tension Mechanical Performance of Martensitic Advanced High Strength Steel Resistance Spot Welds,” *Metall Mater Trans A Phys Metall Mater Sci*, vol. 52, no. 2, pp. 655–667, 2021, doi: 10.1007/s11661-020-06104-5.
[20] M. Piott, A. Werber, L. Schleuss, N. Doynov, R. Ossenbrink, and V. G. Michailov, “A study of the heat transfer mechanism in resistance spot welding of aluminum alloys AA5182 and AA6014,” *International Journal of Advanced Manufacturing Technology*, vol. 111, no. 1–2, pp. 263–271, Nov. 2020, doi: 10.1007/s00170-020-05650-x.
[21] S. Zhang, “Fracture mechanics solutions to spot welds,” 2001.
[22] M. Ali, D. Porter, J. Kömi, M. Eissa, H. El Faramawy, and T. Mattar, “Effect of cooling rate and composition on microstructure and mechanical properties of ultrahigh-strength steels,” *Journal of Iron and Steel Research International*, vol. 26, no. 12, pp. 1350–1365, Dec. 2019, doi: 10.1007/s42243-019-00276-0.
[23] V. Javaheri, A. Pohjonen, J. I. Asperheim, D. Ivanov, and D. Porter, “Physically based modeling, characterization and design of an induction hardening process for a new slurry pipeline steel,” *Mater Des*, vol. 182, Nov. 2019, doi: 10.1016/j.matdes.2019.108047.
[24] Z. Han, J. Orozco, J. E. Indacochea, and C. H. Chen, “Resistance spot welding: a heat transfer study,” *Welding Journal (Miami, Fla)*, vol. 68, no. 9, 1989.
[25] H. M. Mallaradhya, M. Vijay Kumar, R. Ranganatha, S. Darshan, and Lochan, “Resistance spot welding: A review,” Apr. 30, 2018, *Transstellar Journal Publications and Research Consultancy Private Limited (TJPRC)*. doi: 10.24247/ijmperdapr201846.
[26] T. K. Pal and K. Chattopadhyay, “Resistance spot weldability and high cycle fatigue behaviour of martensitic (M190) steel sheet,” *Fatigue Fract Eng Mater Struct*, vol. 34, no. 1, pp. 46–52, Jan. 2011, doi: 10.1111/j.1460-2695.2010.01489.x.
[27] A. Chabok, E. van der Aa, I. Basu, J. De Hosson, and Y. Pei, “Effect of pulse scheme on the microstructural evolution, residual stress state and mechanical performance of resistance spot welded DP1000-GI steel,” *Science and Technology of Welding and Joining*, vol. 23, no. 8, pp. 649–658, 2018, doi: 10.1080/13621718.2018.1452875.
[28] G. H. Farrahi, A. Ahmadi, and K. Reza Kasyzadeh, “Simulation of vehicle body spot weld failures due to fatigue by considering road roughness and vehicle velocity,” *Simul Model Pract Theory*, vol. 105, Dec. 2020, doi: 10.1016/j.simpat.2020.102168.

[29] M. Mansouri, H. Abadi, and M. Pouranvari, “Failure-Mode Transition in Resistance Spot welded DP780 Advanced High-Strength Steel: Effect of Loading Conditions,” *Materiali in tehnologije*, vol. 48, no. 1, pp. 67–71, Apr. 2014.

[30] J. J. F. Bonnen *et al.*, “Fatigue of Advanced High Strength Steel Spot-Welds,” 2006.

[31] I. A. Soomro, S. R. Pedapati, and M. Awang, “A review of advances in resistance spot welding of automotive sheet steels: emerging methods to improve joint mechanical performance,” *International Journal of Advanced Manufacturing Technology*, vol. 118, no. 5–6, pp. 1335–1366, 2022, doi: 10.1007/s00170-021-08002-5.

[32] L. Shi, J. Kang, M. Gesing, X. Chen, A. S. Haselhuhn, and B. E. Carlson, “Effect of notch root angle on fatigue behavior of aluminum to steel resistance spot welds,” *Int J Fatigue*, vol. 141, Dec. 2020, doi: 10.1016/j.ijfatigue.2020.105866.

[33] C. Wei and H. T. Kang, “Fatigue life prediction of spot-welded joints with a notch stress approach,” *Theoretical and Applied Fracture Mechanics*, vol. 106, Apr. 2020, doi: 10.1016/j.tafmec.2020.102491.

[34] B. Pal, M. Amirthalingam, and S. G. S. Raman, “An Experimental Investigation on the High Cycle Fatigue Behavior of Resistance Spot Welded Ultrahigh Strength Steel,” *J Mater Eng Perform*, Dec. 2023, doi: 10.1007/s11665-023-08914-1.

[35] R. W. Rathbun, “Fatigue Behavior of Spot Welded High Strength Sheet Steels,” 2018.

[36] E. Bayraktar, D. Kaplan, F. Schmidt, H. Paqueton, and M. Grumbach, “State of art of impact tensile test (ITT): Its historical development as a simulated crash test of industrial materials and presentation of new ‘ductile/brittle’ transition diagrams,” *J Mater Process Technol*, vol. 204, no. 1–3, pp. 313–326, Aug. 2008, doi: 10.1016/j.jmatprotec.2007.11.044.

[37] C. Jurewicz, A. Sobhani, J. Woolley, J. Dutschke, and B. Corben, “Exploration of Vehicle Impact Speed – Injury Severity Relationships for Application in Safer Road Design,” *Transportation Research Procedia*, vol. 14, pp. 4247–4256, 2016, doi: 10.1016/j.trpro.2016.05.396.

[38] R. Muscat and M. Mahfouf, “Predicting Charpy Impact Energy for Heat-Treated Steel using a Quantum-Membership-Function-based Fuzzy Model,” in *IFAC-PapersOnLine*, Elsevier B.V., 2016, pp. 138–142. doi: 10.1016/j.ifacol.2016.10.110.

[39] E. Bayraktar, J. Chevalier, F. Bonnet, D. Kaplan, and J. Claeys, “Impact tensile test: A new type of crash test for welded joints used in automotive applications,” EDP Sciences, 2009, pp. 235–241. doi: 10.1051/dymat/2009032.

[40] J. Dong, J. Hu, and Z. Luo, “Quality Monitoring of Resistance Spot Welding Based on a Digital Twin,” *Metals (Basel)*, vol. 13, no. 4, Apr. 2023, doi: 10.3390/met13040697.

[41] D. Zhao, N. Vdonin, M. Slobodyan, S. Butsykin, A. Kiselev, and A. Gordynets, “Assessing Electrode Characteristics in Continuous Resistance Spot Welding of BH 340 Steel Based on Dynamic Resistance,” *Journal of Manufacturing and Materials Processing*, vol. 7, no. 6, Dec. 2023, doi: 10.3390/jmmp7060218.

[42] J. Stephen, “Spot Weld Examination using NDE Methods,” 2019. [Online]. Available: http://www.ndt.net/?id=25726